

# AN EFFICIENT METHOD FOR BAND STRUCTURE CALCULATIONS IN 2D PHOTONIC CRYSTALS

DAVID C. DOBSON\*

**Abstract.** An efficient method for band structure calculations in dielectric photonic crystals is presented. The method uses a finite element discretization coupled with a preconditioned subspace iteration algorithm. Numerical examples are presented which illustrate the behavior of the method.

**1. Introduction.** Photonic crystals are periodic structures composed of dielectric materials and designed to exhibit interesting properties, such as spectral band gaps, in the propagation of classical electromagnetic waves. Structures with band gaps have many potential applications, for example in optical communications, filters, lasers, and microwaves. See [2, 13] for an introduction to photonic crystals. Figotin and Kuchment have proved that periodic dielectric structures exist which exhibit band gaps [9, 10], and other band gap structures have been found through computational and physical experiments. Computation has become a primary tool for investigating the properties of these structures.

Carrying out a complete band structure calculation for a given photonic crystal generally involves solving a large family of eigenproblems, as the *quasimomentum* parameter (defined in the next section) is varied over the first Brillouin zone. Solving this set of eigenproblems can be a computational burden, even for a single given photonic crystal. The computational cost is greatly multiplied in optimal design situations, where one wishes to evaluate a large number of structures in order to find one with some optimal property.

In this paper we describe a method which is well suited for efficient band structure calculations in photonic crystals. Here we consider only “two-dimensional” structures. The central building block of our approach is a subspace preconditioning method for general symmetric eigenproblems studied by Bramble, Knyazev, and Pasciak [3]. Our method combines the subspace preconditioning algorithm with a simple finite element discretization of the original family of eigenproblems, and a fast Fourier transform preconditioner. The subspace preconditioning algorithm is an iterative method which takes a given approximate eigen-subspace and iteratively improves it. This makes the method very efficient for solving continuously varying families of problems, as in band structure calculations. Small changes in the parameter generally result in small changes in the associated eigen-subspace, so that the subspace from a previous solve can be used as an accurate estimate for the next parameter value. Further efficiency is gained through the use of a preconditioner. Our preconditioner is most effective for structures composed of “low-contrast” mixtures of materials. In the optical frequency range, the contrast between the refractive indices  $k_1$ ,  $k_2$  of two typical dielectric materials

---

\* Department of Mathematics, Texas A&M University, College Station, TX 77843-3368. [dobson@math.tamu.edu](mailto:dobson@math.tamu.edu). Research supported by AFOSR grant number F49620-98-1-0005 and Alfred P. Sloan Research Fellowship.

is generally relatively low (say  $k_1/k_2 \leq 3$ ). In this parameter regime, the method is efficient enough to apply in an optimal design setting [5].

Many other methods have been developed for the computation of band structures in photonic crystals, both 2D and 3D. Most previous methods which allow for general dielectric structures are based on natural truncated plane wave decompositions of the fields (see eg. the survey [2] and the references therein). While acceptable accuracy can be obtained with these methods, it is often at a large computational cost, due to the slow convergence of the truncated field in media with sharp discontinuities. Alternative methods such as the T-matrix and R-matrix methods have been proposed, and are based on calculating a transfer matrix for Maxwell's equations. Such propagation methods are particularly useful for calculations in truncated structures. A comparison of the T-matrix and R-matrix approaches can be found in [7]. A method designed specifically for band structure calculations in certain crystal configurations which are known to produce band gaps has been developed by Figotin and Godin [8]. This method is highly efficient even for materials with large contrasts.

Finally, Axmann and Kuchment [1] have recently proposed a finite element method for band structure calculations in 2D photonic crystals. Their basic approach is similar to the method described here, but different in two main respects. First, their finite element approximation scheme uses general unstructured grids, where the method presented here uses a uniform, rectangular grid. Rectangular grids are easier to implement, but unstructured grids generally offer a more accurate field approximation using fewer grid points. The second main difference is the method of solution for the discrete eigenproblems. Our approach uses a fast approximate solution operator as a preconditioner, which is embedded within the subspace iterations, and which makes use of the fact that the grid is rectangular. Axmann and Kuchment use a simultaneous coordinate over-relaxation method, which does not require the use of an approximate solution operator. Each approach presents certain advantages and disadvantages; perhaps further work will produce new methods achieving the best features of both.

Extension of the finite element approach to the full Maxwell equations in 3D photonic crystals is work in progress. Finite element techniques for typical 3D electromagnetics problems in engineering are well developed [12]. Also, the efficiency of the solution methods described here and in [1] for 2D problems is very favorable for large problems. Our hope is that by coupling known 3D finite element discretization techniques with a fast solution algorithm, an effective method for 3D photonic crystals will result.

The outline of the remainder of this paper is as follows. In the following section, we formulate the discrete finite element problem. Then in Section 3, we introduce a fast Fourier transform (FFT) preconditioner. In Section 4, we describe the subspace preconditioning algorithm. Finally in Section 5 we numerically illustrate some of the properties of the method.

**2. Problem formulation.** Beginning with Maxwell's equations

$$(1) \quad \nabla \times E - i\omega\mu H = 0, \quad \nabla \times H + i\omega\epsilon E = 0,$$

we assume that the magnetic permeability  $\mu$  is constant, and the medium is orthotropic, that is, the dielectric tensor  $\epsilon$  can be written

$$(2) \quad \epsilon = \begin{pmatrix} \epsilon_{11} & \epsilon_{12} & 0 \\ \epsilon_{21} & \epsilon_{22} & 0 \\ 0 & 0 & \epsilon_{33} \end{pmatrix}.$$

We assume that all material properties are constant in the  $x_3$  direction, that  $\epsilon$  is positive definite, and that  $\epsilon_{12} = \epsilon_{21}$ . In the  $E$ -parallel case, where the electric field is given by  $E = (0, 0, u)$ , equations (1) then reduce to

$$(3) \quad \Delta u + \omega^2 \rho u = 0, \quad \text{in } \mathbb{R}^2,$$

where  $\rho(x) = \mu \epsilon_{33}(x)$ ,  $x = (x_1, x_2)$ . In the  $H$ -parallel case, where the magnetic field is given by  $H = (0, 0, u)$ , equations (1) reduce to

$$(4) \quad \nabla \cdot (M \nabla u) + \omega^2 u = 0, \quad \text{in } \mathbb{R}^2,$$

where the matrix  $M(x)$  is given by

$$(5) \quad M = \frac{1}{\mu(\epsilon_{11}\epsilon_{22} - \epsilon_{12}^2)} \begin{pmatrix} \epsilon_{22} & -\epsilon_{12} \\ -\epsilon_{12} & \epsilon_{11} \end{pmatrix}.$$

We assume that the structure has unit periodicity on a square lattice. Thus denoting  $Z = \{0, \pm 1, \pm 2, \dots\}$ , and defining the lattice  $\Lambda = Z^2$ , we assume that

$$\epsilon(x + n) = \epsilon(x), \quad \text{for all } x \in \mathbb{R}^2, \text{ and for all } n \in \Lambda.$$

We define the periodic domain

$$\Omega = \mathbb{R}^2 / Z^2,$$

which can be identified with the unit square  $(0, 1)^2$  with periodic boundary conditions. Define the first Brillouin zone  $K = [-\pi, \pi]^2$ . To reduce the problem over  $\mathbb{R}^2$  to a family of problems over  $\Omega$ , one defines for  $g \in L^2(\mathbb{R}^2)$  the Floquet transform

$$(\mathcal{F}g)(\alpha, x) = e^{-i\alpha \cdot x} \sum_{n \in Z^2} g(x - n) e^{i\alpha \cdot n}, \quad \alpha \in K.$$

The sum can be considered as a Fourier series in the *quasimomentum* variable  $\alpha$ , with values in  $L^2(\Omega)$ ; see [14] for details.

Formally,  $(\nabla + i\alpha)\mathcal{F}g = \mathcal{F}(\nabla g)$ , where the gradient is with respect to the  $x$  variable. Under the mapping  $\mathcal{F}$ , the  $E$ -parallel problem (3) transforms to

$$(6) \quad (\nabla + i\alpha) \cdot (\nabla + i\alpha) u_\alpha + \omega^2 \rho u_\alpha = 0 \quad \text{in } \Omega, \quad \alpha \in K,$$

where  $u_\alpha$  is the Floquet transform of  $u$ . Similarly, the  $H$ -parallel problem (4) transforms to

$$(7) \quad (\nabla + i\alpha) \cdot M(\nabla + i\alpha) u_\alpha + \omega^2 u_\alpha = 0 \quad \text{in } \Omega, \quad \alpha \in K.$$

For notational simplicity, from now on we drop the subscript  $\alpha$  when referring to  $u$ .

Let  $H^1(\Omega)$  denote the usual Sobolev space of square integrable functions with square integrable first-order derivatives. The natural variational eigenproblems associated with (6) and (7) are, respectively,

$$(8) \quad a_\alpha(1; u, v) = \omega^2 b(\rho; u, v), \quad \text{for all } v \in H^1(\Omega) \quad (E\text{-parallel})$$

and

$$(9) \quad a_\alpha(M; u, v) = \omega^2 b(1; u, v), \quad \text{for all } v \in H^1(\Omega) \quad (H\text{-parallel})$$

where

$$\begin{aligned} a_\alpha(M; u, v) &= \int_{\Omega} M(\nabla + i\alpha)u \cdot \overline{(\nabla + i\alpha)v} \\ b(\rho; u, v) &= \int_{\Omega} \rho u \bar{v}. \end{aligned}$$

The quadratic forms  $a_\alpha$  and  $b$  are Hermitian.

Discrete versions of the variational problems (8), (9) are then obtained in the standard way by introducing for a given ‘‘discretization level’’  $N$ , an approximating subspace  $S_N \subset H^1(\Omega)$ . Problem (8) is then replaced by the discrete problem: find nonzero  $u_N \in S_N$  and  $\omega^2$  such that

$$(10) \quad a_\alpha(1; u_N, \phi) = \omega^2 b(\rho; u_N, \phi), \quad \text{for all } \phi \in S_N,$$

and similarly for the  $H$ -parallel polarization case (9).

In our implementation, due to the simple geometry of the domain  $\Omega$ , and our wish to maintain as much symmetry as possible in the discrete problem, we choose  $S_N$  to be composed of piecewise-bilinear nodal finite elements on a uniform  $\sqrt{N} \times \sqrt{N}$  square grid. Convergence properties for finite element approximations for similar elliptic eigenvalue problems are well-known, see for example [4]. For both problems (8) and (9), the finite element approximations are convergent, assuming only that  $\epsilon$  is bounded, measurable, and uniformly bounded away from zero. However, for problem (8), the convergence is generally faster, essentially due to the better smoothness properties of eigenvectors  $u$ . Our focus here is not on the convergence of the discrete approximations  $u_N$  as  $N \rightarrow \infty$ , although some numerical examples are given in Section 5.2.

Given the standard set of nodal basis elements  $\{\phi_j\}_{j=1}^N \subset S_N$ , we write (10) as a matrix eigenproblem

$$(11) \quad A_\alpha^E u = \omega^2 B^E u, \quad (E\text{-parallel})$$

where the entries of the matrices are given by

$$(A_\alpha^E)_{jk} = a_\alpha(1; \phi_j, \phi_k), \quad (B^E)_{jk} = b(\rho; \phi_j, \phi_k), \quad 1 \leq j, k \leq N,$$

and now  $u$  is a vector representing the approximate eigenfunction in terms of the basis  $\{\phi_j\}$ . The matrix problem corresponding to the  $H$ -parallel case (9) will be written

$$(12) \quad A_\alpha^H u = \omega^2 B^H u, \quad (H\text{-parallel})$$

where

$$(A_\alpha^H)_{jk} = a_\alpha(M; \phi_j, \phi_k), \quad (B^H)_{jk} = b(1; \phi_j, \phi_k), \quad 1 \leq j, k \leq N,$$

In our implementation, the integrals  $b(\rho; \phi_j, \phi_k)$  and  $a_\alpha(M; \phi_j, \phi_k)$  are calculated explicitly by assuming that  $\rho$  and  $M$  are piecewise constant over the grid.

**3. Preconditioner.** Due to the periodic geometry, the differential operator

$$L_\alpha = -(\nabla + i\alpha) \cdot (\nabla + i\alpha) = -\Delta - 2i\alpha \cdot \nabla + |\alpha|^2$$

is easily separable in terms of Fourier coefficients. Specifically, writing

$$f(x) = \sum_{n \in \Lambda} f_n e^{2\pi i n \cdot x}, \quad \text{where } f_n = \int_{\Omega} f(x) e^{-2\pi i n \cdot x} dx,$$

we see that

$$(13) \quad L_\alpha f = \sum_{n \in \Lambda} |2\pi n + \alpha|^2 f_n e^{2\pi i n \cdot x},$$

where the sum is interpreted in a weak sense if necessary. Note that for  $\alpha \in K = [-\pi, \pi]^2$ , the term  $|2\pi n + \alpha|$  is zero only when  $n = \alpha = 0$ . Consequently, one has an explicit representation for the inverse (modulo constants in the  $\alpha = 0$  case),

$$(14) \quad L_\alpha^{-1} f = \sum_{\substack{n \in \Lambda \\ 2\pi n + \alpha \neq 0}} |2\pi n + \alpha|^{-2} f_n e^{2\pi i n \cdot x}.$$

Our approach uses this representation to obtain a preconditioner, i.e., an approximate inverse, for the finite element discretization described in the previous section. In the discrete setting, an approximation to  $L_\alpha^{-1}$  can be calculated very efficiently using the fast Fourier transform. Specifically, if  $F$  denotes the FFT operation on a sampled grid function on a  $\sqrt{N} \times \sqrt{N}$  uniform grid, we can define

$$S_\alpha = F^{-1} D_\alpha F,$$

where  $D_\alpha$  is a diagonal scaling matrix with entries  $|2\pi n + \alpha|^{-2}$  on the diagonal.  $S_\alpha$  can be viewed as a discrete approximation to  $L_\alpha^{-1}$ . Since  $S_\alpha$  is not constructed in the same finite element space as the matrix  $A_\alpha^E$ , it will not be an exact matrix inverse. For our purposes,  $S_\alpha$  will be used only as an *approximate* inverse for the matrix  $A_\alpha^E$  (as well as for  $A_\alpha^H$ ). Notice that calculating the product  $S_\alpha v$ , for any  $N$ -vector  $v$ , is a  $\mathcal{O}(N \log N)$  operation.

**4. Subspace preconditioning algorithm.** The algorithm we propose for solving the matrix eigenvalue problems (11) and (12) is a trivial modification of a method studied by Bramble, Pasciak, and Knyazev [3] (the modification is to handle generalized eigenproblems). The idea of using preconditioned iterations for computing eigenvalues is not new, dating back at least to Samokish [16] and Petryshyn [15]. Convergence

analysis in the case of one eigenvalue was done by Godunov et al [11]. The basic iteration used here was studied by D'yakonov and Orekhov [6]. In addition, several alternative preconditioned schemes have since been proposed to further enhance the convergence of the basic iteration; see the references in [3] for details.

Let us denote problems (11) and (12) generically by

$$A_\alpha u = \lambda B u.$$

The preconditioned subspace iteration algorithm is intended to find a relatively small number, say  $s$ , of the smallest eigenvalues in large-dimensional symmetric positive definite matrix problems. The basic method develops a sequence of approximating eigenspaces

$$V_s^n = \text{span}\{v_1, \dots, v_s\} \quad n = 1, 2, \dots$$

Applied to our band structure calculation problem, the method proceeds as follows. First, choose an initial subspace  $V_s^0$ . A space spanned by  $s$  pseudo-random, linearly independent  $N$ -vectors usually suffices. Next, for  $n = 0, 1, 2, \dots$ , perform the iteration:

1. Compute the Ritz eigenvectors  $\{v_j^n\}_{j=1}^s \subset V_s^n$ , and their corresponding eigenvalues  $\lambda_1^n \leq \lambda_2^n \leq \dots \leq \lambda_s^n$  satisfying

$$\langle A_\alpha v_j^n, w \rangle = \lambda_j^n \langle B v_j^n, w \rangle, \quad \text{for all } w \in V_s^n.$$

2. Compute

$$\hat{v}_j^{n+1} = v_j^n - S_\alpha(A_\alpha v_j^n - \lambda_j^n B v_j^n), \quad \text{for } j = 1, \dots, s.$$

3. Define  $V_s^{n+1} = \text{span}\{\hat{v}_1^{n+1}, \dots, \hat{v}_s^{n+1}\}$ .

Most of the work in each iteration is expended computing the matrix-vector products  $A_\alpha v_j^n$ ,  $B v_j^n$ ,  $j = 1, \dots, s$ . With the finite element discretization described Section 2,  $A_\alpha$  and  $B$  essentially have only nine nonzero diagonals, so each matrix-vector product is an  $O(N)$  operation. Computing the action of the preconditioner  $S_\alpha$  on a vector is an  $O(N \log N)$  operation. Thus with  $s$  fixed, each iteration of steps (1-3) requires  $O(N \log N)$  time. It is important to note that the Ritz eigenproblem in step 1 is  $s$ -dimensional, so that for small  $s$  (typically  $s \approx 10$ ), this is a trivial amount of work. The iteration (1-3) can be terminated for example when  $\max_j \{|\lambda_j^n - \lambda_j^{n+1}|\}$  is less than some desired tolerance.

Estimates which, under certain assumptions on the preconditioner, prove that the subspace iteration converges at a rate which is *independent of the grid size* are provided in [3]. In the next section we will investigate numerically some of the convergence properties of the algorithm.

To do a full band structure calculation, one can now proceed in the obvious way, sampling quasimomentum vectors  $\alpha$  in the first Brillouin zone with a finite number of  $\alpha_k$ , and solving each eigenproblem with the algorithm above, one  $k$  at a time. In practice, by choosing the sequence  $\{\alpha_k\}$  so that each distance  $|\alpha_k - \alpha_{k+1}|$  is small, one gets a good approximate subspace  $V_s^0$  for the  $(k+1)$ st problem by using the final subspace  $V_s^n$  from the  $k$ th problem. Typically after the first problem is solved, each additional problem requires only a few subspace preconditioning iterations.

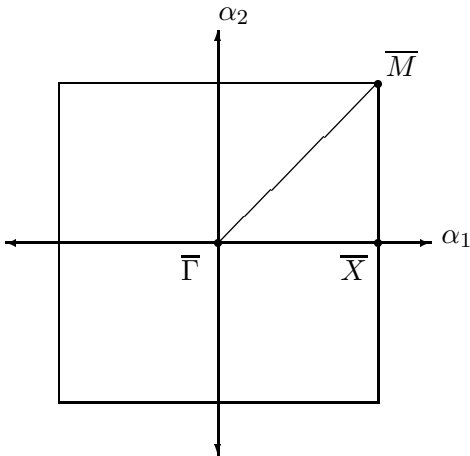
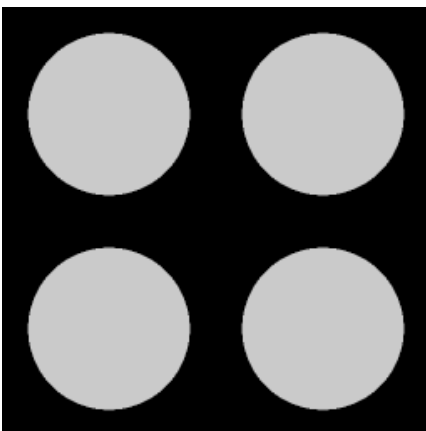


FIG. 1. First Brillouin zone and symmetry points  $\bar{\Gamma}$ ,  $\bar{X}$ , and  $\bar{M}$ .

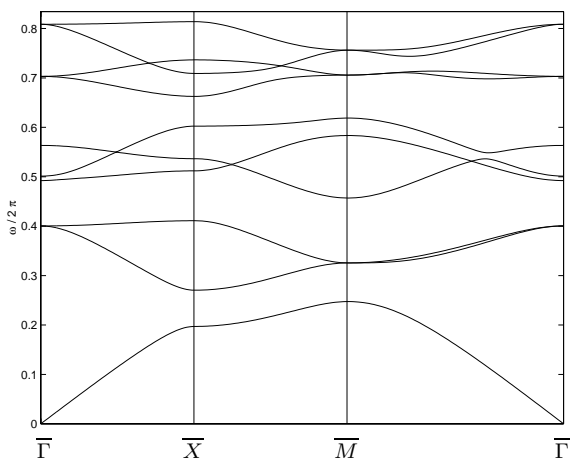
**5. Numerical experiments.** Our goal in this section is to illustrate the performance of the method for typical 2D photonic crystals. The method was implemented entirely in *Matlab*; computations were carried out on a Sun UltraSparc workstation. We begin this section by presenting two simple band structure calculations.

**5.1. Examples.** A typical band structure calculation proceeds by computing the first  $s$  eigenvalues for various values of  $\alpha$ , as  $\alpha$  is varied along lines between points of high symmetry in the first Brillouin zone, as shown in Figure 1. Alternatively, a density of states calculation can be done by sampling many values of  $\alpha$  in the first Brillouin zone and counting corresponding states in specified frequency ranges. A simple band calculation example is shown in Figure 2. In this example, the photonic crystal is an array of circular isotropic rods, as pictured in Figure 2(a). The rods have high dielectric constant ( $\epsilon = 8.9$ ) and are surrounded by air ( $\epsilon = 1$ ). Band structures in  $E$ - and  $H$ -parallel polarization modes are shown in Figures 2(b) and 2(c), respectively. The computations were carried out on a  $64 \times 64$  grid, and required roughly a half-hour of wall-clock time.

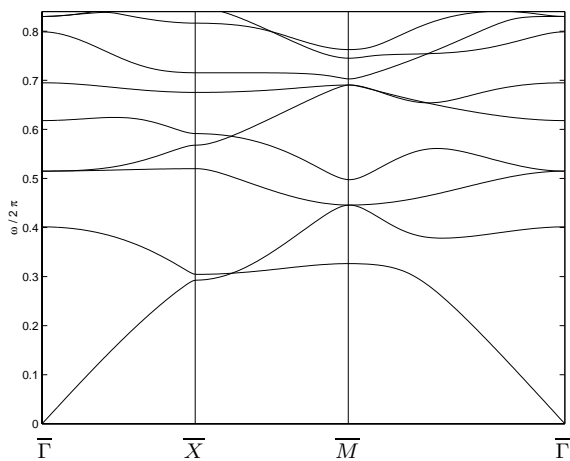
In the next example, we consider anisotropic media. As is well-known, this situation arises naturally when considering “layered” composite structures, such as the one pictured in Figure 3(a). Such structures would of course be of most interest at larger-than-optical length scales, where fabrication is more plausible. In the figure, light areas represent an isotropic material with  $\epsilon = 17$  and dark areas represent an isotropic material with  $\epsilon = 1$ . One could of course retain the isotropic problem and compute directly with the structure in Figure 3(a). However, if one wishes to increase the number of layers in each “slab” while holding its thickness fixed, then the grid must be refined, which can become a computational burden. By instead passing to the limit as the number of layers becomes infinite and applying effective media theory, one obtains an orthotropic problem. In the effective orthotropic problem, each vertical slab becomes a



(a) Four cells of circular rod structure. Light-shaded area represents  $\epsilon = 8.9$ , dark area has  $\epsilon = 1$ .



(b)  $E$ -parallel polarization



(c)  $H$ -parallel polarization

FIG. 2. Computed band structure for circular dielectric rod of radius 0.378, where the cell side length is one.

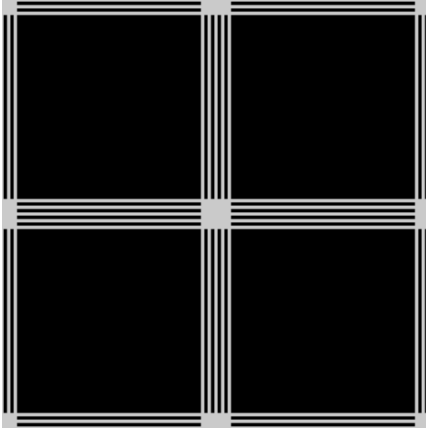
homogeneous composite material with

$$\epsilon = \begin{pmatrix} 9 & 0 & 0 \\ 0 & \frac{17}{9} & 0 \\ 0 & 0 & 9 \end{pmatrix}.$$

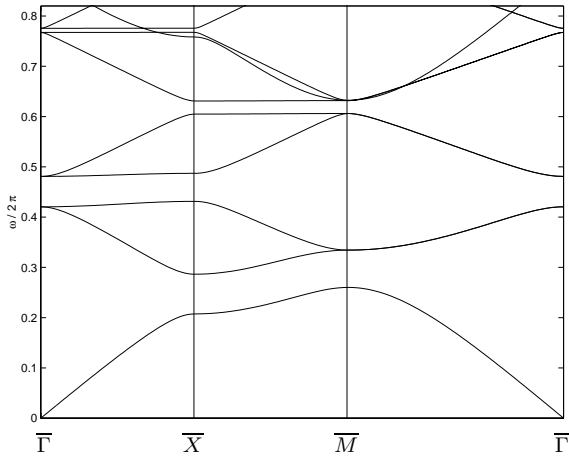
Similarly, each horizontal slab is homogeneous, with  $\epsilon$  as above, but with  $\epsilon_{11}$  and  $\epsilon_{22}$  reversed. The band structure corresponding to this effective media model was calculated on a  $64 \times 64$  grid and is shown in Figures 3(b) and (c). It was found to differ very little from the band structure obtained by direct computation on the layered isotropic model with a finer grid.

**5.2. Convergence of finite element approximations.** In the  $E$ -parallel case, standard convergence estimates (see eg. [4]) indicate that finite element solutions, using piecewise bilinear elements as in our implementation, are linearly convergent to exact solutions as the grid spacing is reduced. A numerical check of this estimate is shown in Figure 5, where we plot the maximum difference between the first five eigenvalues, computed on  $m \times m$  and  $\frac{m}{2} \times \frac{m}{2}$  grids. This check is carried out on two different photonic crystals: the first is the circular dielectric rod structure shown in Figure 2(a), and the second is a similar dielectric rod structure with a square cross section and side length 0.5, shown in Figure 4. The computational results are consistent with linear convergence in both cases, and also agree with the type of convergence behavior observed by Axmann and Kuchment [1]. In  $H$ -parallel polarization, it can be proved that the finite element approximation is convergent, but for arbitrary  $\epsilon(x)$  one cannot expect a definite convergence rate. In Figure 5(a) we see that convergence in  $H$ -parallel mode appears to be less than linear for the circular dielectric rod structure. Some improvement could be obtained by implementing more accurate integration rules; recall from Section 2 that in our implementation, the matrix entries (12) are calculated assuming a piecewise constant dielectric coefficient. For structures in which jumps in the dielectric coefficient are aligned with the computational grid, as in the square rod example, the integration rules are exact and the grid conforms naturally with the regularity of the eigenfunctions. Consequently, convergence is better, as shown in Figure 5(b).

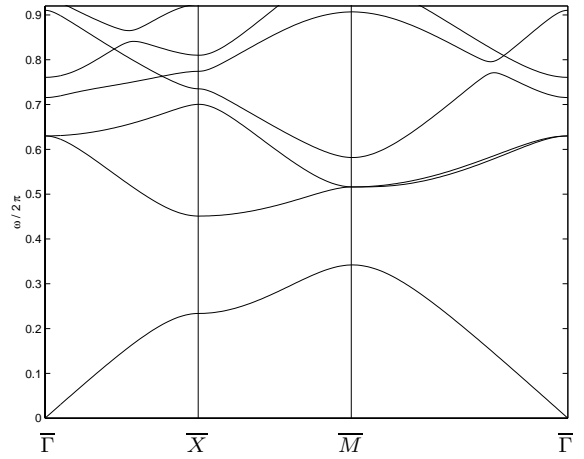
**5.3. Convergence of subspace iterations.** In practice, the number of preconditioned subspace iterations required to reach a given tolerance in  $\max_j \{|\lambda_j^n - \lambda_j^{n+1}|\}$  is at worst a very slowly growing function of the grid size  $N$ . This is difficult to check numerically, because a primary factor determining the number of iterations required on a subspace of a given dimension  $s$  is the distance between the largest eigenvalue  $\lambda_s$  within the subspace and the smallest eigenvalue  $\lambda_{s+1}$  outside the subspace. As  $N$  is varied, this distance generally changes. However for simple examples chosen such that  $|\lambda_s - \lambda_{s+1}|$  is relatively insensitive to  $N$ , we can get a qualitative idea of the general behavior. For a series of computations in which the first three bands in  $E$ -parallel polarization of the square rod structure shown in Figure 4 were calculated to a stopping tolerance of  $\max_j \{|\lambda_j^n - \lambda_j^{n+1}|\} < 5 \times 10^{-6}$ , the average number of subspace iterations per solve grows monotonically, but slowly, from 5.7 iterations for  $N = 256$  to 6.1 iterations at



(a) Four cells of layered structure. Light-shaded area represents  $\epsilon = 17$ , dark area has  $\epsilon = 1$ .



(b)  $E$ -parallel polarization



(c)  $H$ -parallel polarization

FIG. 3. Computed band structure for (anisotropic) effective medium limit of layered structure. Note that gaps appear in both  $E$ - and  $H$ -parallel modes.

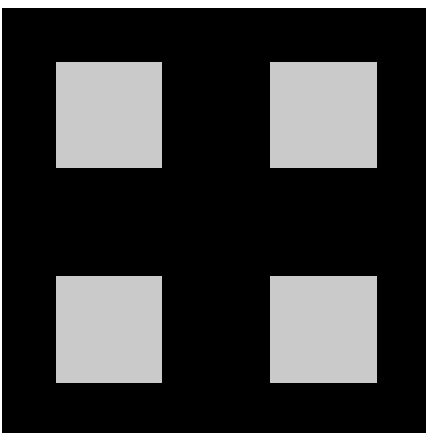
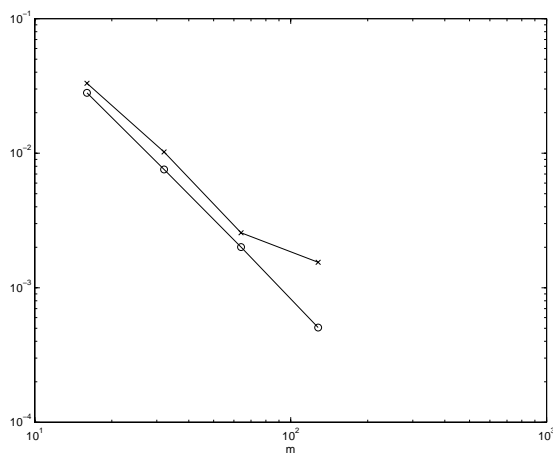
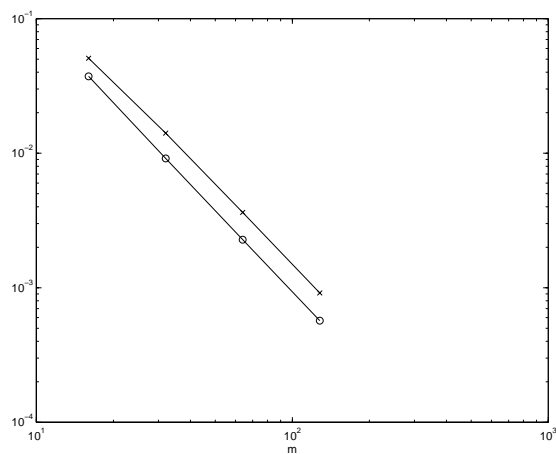


FIG. 4. Square rod structure used for convergence checks. Rod side length is 0.5, dielectric coefficient in rod (shaded light) is  $\epsilon = 8.9$ , surrounding medium is  $\epsilon = 1$ .



(a) Circular dielectric rod structure.



(b) Square dielectric rod structure.

FIG. 5. Maximum difference in first five computed eigenvalues  $\max_j |\lambda_j^m - \lambda_j^{m/2}|$ , where  $\lambda_j^m$  is the  $j$ th eigenvalue computed on an  $m \times m$  grid, versus linear grid size  $m$ . Circles indicate  $E$ -parallel mode; crosses indicate  $H$ -parallel mode.

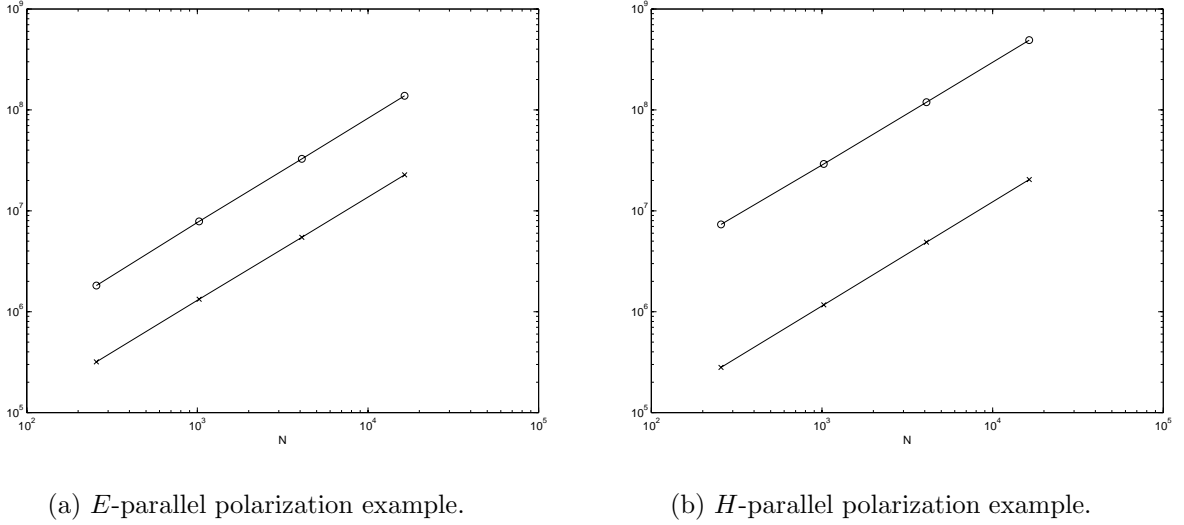


FIG. 6. Number of floating point operations versus grid size  $N$ . Circles represent average number of operations per solve. Crosses represent average number of operations per preconditioned subspace iteration.

$N = 16384$ . Furthermore, as illustrated in Figure 6(a), the amount of work required for the complete band calculation (measured in number of floating point operations) scales roughly like  $N \log N$ , the same as a single preconditioned subspace iteration.

The preconditioner is generally not as effective in the  $H$ -parallel polarization case as it is in  $E$ -parallel polarization. Hence each solve requires more subspace iterations. In a series of computations similar to the last example, but in  $H$ -parallel polarization, the average number of subspace iterations per solve was larger, but actually decreased monotonically from 26.1 iterations per solve at  $N = 256$ , to 24.1 iterations per solve at  $N = 16384$ . Average work per solve and per step increased “almost” linearly with  $N$ , as illustrated in Figure 6(b).

A key factor determining the effectiveness of the preconditioner is the contrast between dielectric coefficients of the materials which compose the photonic crystal. Generally, the preconditioner works better for small contrast. The effect of the preconditioner on convergence of the subspace iteration is complicated, but can be examined qualitatively by looking at the step

$$\hat{v}_j^{n+1} = v_j^n - S_\alpha(A_\alpha v_j^n - \lambda_j^n B v_j^n).$$

Roughly speaking, if the quantity

$$(15) \quad \gamma(\lambda) = \|S_\alpha(A_\alpha - \lambda B)\|,$$

is small, then the update to the approximate eigenvector  $\hat{v}_j^{n+1}$  is small, and the iteration converges more rapidly. The behavior of  $\gamma(\lambda)$  is different for  $E$ - and  $H$ -parallel modes, but always increases with the contrast. Figure 7 shows various values of  $\gamma(\lambda)$  as the contrast of the dielectric rod structure is increased from  $\epsilon = 1$  to  $\epsilon = 20$ . Obviously the

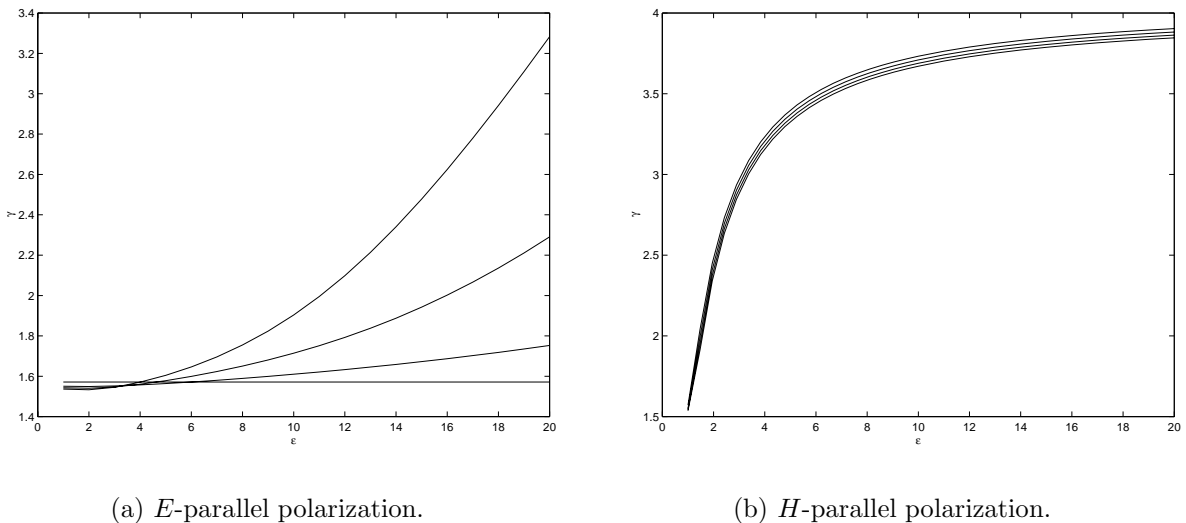


FIG. 7. The quantity  $\gamma(\lambda)$ , defined in (15), for  $\lambda = 0, \frac{1}{3}, \frac{2}{3}, 1$ . The horizontal axis represents the contrast in material parameters for the isotropic dielectric rod structure in Figure 2.

*E*-parallel mode behaves better in the optical contrast range  $\epsilon \approx 9$ . This helps explain the improved convergence we observed in *E*-parallel mode in the numerical examples. Note however that the *H*-parallel mode appears to have better asymptotic behavior for large contrast.

**6. Conclusions.** We have presented an efficient method for performing band structure calculations in “two-dimensional” photonic crystals. The method uses a finite element discretization coupled with a preconditioned subspace iteration algorithm to solve the discrete eigenproblems. The method can be applied to very general dielectric structures, including those with anisotropic media. The method is most efficient for photonic crystals composed of low-contrast media. Numerical experiments indicate that the computational work required per solve is  $\mathcal{O}(N \log N)$ , where  $N$  is the number of points in the discretization. The basic approach can in principle be extended to handle three-dimensional structures, and more general periodic geometries.

**Acknowledgments.** The author wishes to thank W. Axmann and P. Kuchment for several helpful discussions, and M. Flanagan for programming assistance.

Acknowledgment and Disclaimer: Effort sponsored by the Air Force Office of Scientific Research, Air Force Materiel Command, USAF, under grant number F49620-98-1-0005. The U.S. Government is authorized to reproduce and distribute reprints for Governmental purposes notwithstanding any copyright notation thereon. The views and conclusions contained herein are those of the authors and should not be interpreted as necessarily representing the official policies or endorsements, either expressed or implied, of the Air Force Office of Scientific Research or the U.S. Government.

## REFERENCES

- [1] W. Axmann and P. Kuchment, *A finite element method for computing spectra of photonic and acoustic band-gap materials I. Scalar case*, preprint (1998).
- [2] C. M. Bowden, J. P. Dowling, and H. O. Everitt, editors, *Development and applications of materials exhibiting photonic band gaps*, J. Opt. Soc. Am. B, Vol. 10, No. 2 (1993).
- [3] J. H. Bramble, A. V. Knyazev, and J. E. Pasciak, *A subspace preconditioning algorithm for eigenvector/eigenvalue computation*, Adv. Comp. Math. **6** (1996), 159–189.
- [4] P. G. Ciarlet, *The Finite Element Method for Elliptic Problems*, Elsevier North-Holland, Amsterdam (1978).
- [5] S. J. Cox and D. C. Dobson, *Maximizing band gaps in two-dimensional photonic crystals*, SIAM J. Appl. Math., to appear.
- [6] E. G. D'yakonov and M. Yu. Orekhov, *Minimization of the computational labor in determining the first eigenvalues of differential operators*, Math. Notes **27** (1980), 382–391.
- [7] J. M. Elson and P. Tran, *Coupled-mode calculation with the R-matrix propagator for the dispersion of surface waves on a truncated photonic crystal*, Phys. Rev. B **54**, no. 3, (1996), 1711–1715.
- [8] A. Figotin, and Y. A. Godin, *The computation of spectra of some 2D photonic crystals*, J. Comp. Phys. **136**, (1997), 585–598.
- [9] A. Figotin and P. Kuchment, *Band-gap structure of spectra of periodic dielectric and acoustic media. I. Scalar model*, SIAM J. Appl. Math. **56** (1996), 68–88.
- [10] A. Figotin and P. Kuchment, *Band-gap structure of spectra of periodic dielectric and acoustic media. II. Two-dimensional photonic crystals*, SIAM J. Appl. Math. **56** (1996), 1561–1620.
- [11] S. K. Godunov, V. V. Ogneva, and G. P. Prokopov, *On the convergence of the modified steepest descent method in application to eigenvalue problems*, Trans. Amer. Math. Soc. **2** (1976), 105.
- [12] J. Jin, *The Finite Element Method in Electromagnetics*, Wiley, New York (1993).
- [13] J. D. Joannopoulos, R. D. Meade, and J. N. Winn, *Photonic crystals: molding the flow of light*, Princeton University Press (1995).
- [14] P. Kuchment, *Floquet Theory for Partial Differential Equations*, Birkhäuser, Basel (1993).
- [15] W. V. Petryshyn, *On the eigenvalue problem  $Tu - \lambda Su = 0$  with unbounded and non-symmetric operators  $T$  and  $S$* , Philos. Trans. R. Soc. Math. Phys. Sci. **262** (1968), 413–458.
- [16] B. A. Samokish, *The steepest descent method for an eigenvalue problem with semi-bounded operators*, Izv. Vyssh. Uchebn. Zaved. Mat. **5** (1958), 105–114 (in Russian).